Chapter 9

DYNAMIC EMBEDDED OPTIMIZATION AND SHOOTING METHODS FOR POWER SYSTEM PERFORMANCE ASSESSMENT

Ian A. Hiskens
University of Wisconsin - Madison
hiskens@engr.wisc.edu

Jung-Wook Park
University of Wisconsin - Madison
jungwookpark@ieee.org

Vaibhav Donde
University of Illinois at Urbana-Champaign
donde@ieee.org

Abstract Power system dynamic performance enhancement can often be formulated as a dynamic embedded optimization problem. The associated cost function quantifies performance and involves dynamically evolving state variables. The dynamic model is embedded within the constraints. Power systems form an important example of hybrid systems, with interactions between continuous dynamics and discrete events playing a fundamental role in behavior. However, it is shown that for a large class of problems, the cost function is smooth even though the underlying dynamic response is non-smooth. Complementing this design-oriented optimization framework, techniques for assessing power system performance and vulnerability can often be expressed as boundary value problems, and solved using shooting methods. It is shown that performance limitations are closely related to grazing phenomena. Techniques are presented for determining parameter values that induce limit cycles and grazing.

1.   Introduction

Design processes are inherently optimization problems, involving trade-offs between competing objectives, whilst ensuring constraints are satisfied. Such problems are not always established formally, nevertheless underlying optimization principles apply. Design questions arising from system dynamic behavior can also be thought of in an optimization framework. However, the optimization formulation in this case must capture the processes driving dynamics. This class of problems has come to be known as *dynamic embedded optimization.*

Examples of such problems abound in power systems. System operators are often faced with maximizing transmission utilization subject to stability constraints. Voltage collapse can be prevented by shedding load, but determining the correct amount and location involves trade-offs. Shedding too much load incurs the wrath of consumers, but insufficient shedding may not alleviate the problem. The August 2003 blackout in North America illustrated the potential consequences in the latter case [1].

Even the tuning of traditional controllers such as power system stabilizers (PSSs) involves trade-offs. The role of PSSs is to provide damping, so controller tuning focuses on small-signal conditions. As a consequence, performance during the transient period immediately following a large disturbance may be degraded. PSS output limiters attempt to balance these competing effects. It will be shown later that the tuning of these limiter values can be formulated as a dynamic embedded optimization problem.

In contrast to design, analysis of system dynamics is more aligned with understanding extremes of system behavior. Many analysis questions take the form of boundary value problems, which are solved using shooting methods. Two cases will be considered in the sequel, limit cycles and grazing phenomena.

Limit cycle behavior has been observed in power system operation [2]. Such behavior is usually undesirable, and tends to be induced by interactions between generator controllers. In many cases, linear techniques can be used to identify contributing factors, and to retune controls accordingly [3]. Other cases though are truly nonlinear, and may even involve controller limits, making them non-smooth. An example will be considered in Section 4.1. Often nonlinear limit cycles are unsta-

ble, and partially bound the region of attraction of the stable operating point. Linear analysis techniques are inappropriate in such cases. Also reverse-time simulation is unreliable, because it is common for such limit cycles to have saddle characteristics, i.e., attracting in some directions and repelling in others. However, it will be shown in Section 4.1 that limit cycles (even those that are non-smooth) can be formulated as a boundary value problem, and solved using a shooting method.

Power system dynamic behavior is generally subject to performance constraints that seek to ensure appropriate post-fault response. Otherwise excessive transients may trigger protection devices, outaging items of equipment, and possibly leading to cascading system failure [1]. Bounding cases, where the system trajectory just (tangentially) encounters a performance constraint, separate regions of desirable and undesirable behavior. Such tangential encounters are referred to as *grazing*.

Vulnerability to event triggering can be assessed by comparing given (nominal) parameter values with values that induce grazing. If a sufficient margin exists between actual and grazing values, then dynamic performance is guaranteed. Crucial to this assessment is the ability to determine grazing values. This problem can again be formulated as a boundary value problem. An appropriate shooting method is developed in Section 4.2.

2.   Model

2.1   Hybrid systems

Interactions between continuous dynamics and discrete events are an intrinsic part of power system dynamic behavior. Devices that obey physical laws typically exhibit continuous dynamics; examples include generators and their controllers. On the other hand, event-driven discrete behavior is normally associated with rule-based components. Examples in this latter category include protection devices [4], tap-changing transformers [5] and supervisory control [6]. Limits within physical devices also fall into this category; an event occurs when a controller signal saturates, or a FACTS device encounters its maximum/minimum firing angle.

Power systems therefore provide an important application area for *hybrid systems*, i.e., systems that are characterized by:

- continuous and discrete states

- continuous dynamics

- discrete events, or triggers

- mappings that define the evolution of discrete states at events.

A simplified hybrid system representation has the form

$$\dot{x} = f_\rho(x), \qquad \rho \in \mathcal{P} \tag{9.1}$$

with $x(0) = x_0$, $f_\rho : \mathbb{R}^n \to \mathbb{R}^n$, and $\mathcal{P}$ is some finite index set. An event occurs at time τ, with the system in discrete state $\rho(\tau) = i$, if

$$s_{ij}(x(\tau)) = 0 \tag{9.2}$$

where $s_{ij} : \mathbb{R}^n \to \mathbb{R}$ is the event triggering function. For well defined behavior, it must be assumed that event triggers are encountered transversally[1],

$$\nabla s_{ij}^T \dot{x} = \nabla s_{ij}^T f_i \neq 0 \tag{9.3}$$

that event triggering cannot initiate an infinitely fast switching sequence (chattering)[2], and that accumulation (Zeno) effects do not occur [8]. Under those conditions, event triggering results in

$$\rho(\tau^+) = j \tag{9.4}$$

$$x(\tau^+) = h_{ij}(x(\tau)) \tag{9.5}$$

where τ^+ refers to the time incrementally beyond switching time τ. Equations (9.4)-(9.5) imply that at time τ a transition $f_i \to f_j$ occurs in the governing dynamics, and h_{ij} forces an impulsive step in the state. (No impulse occurs if $h_{ij}(x) = x$ though.) The model induces the system *flow*

$$x(t) = \phi(t, x_0) \tag{9.6}$$

This simple model provides clarity in the development and discussion of subsequent algorithms. However it is generally inadequate for representing power systems. A more elaborate differential-algebraic model, which incorporates switching and impulse effects, is described in [9].

A compact development of optimization and shooting method algorithms results from incorporating parameters $\lambda \in \mathbb{R}^\ell$ into the dynamic states x. (Numerical implementation is also simplified.) This is achieved by introducing trivial differential equations $\dot{\lambda} = 0$ into (9.1), and results in the natural partitioning

$$x = \begin{bmatrix} \underline{x} \\ \lambda \end{bmatrix}, \qquad f = \begin{bmatrix} \underline{f} \\ 0 \end{bmatrix}, \qquad h_j = \begin{bmatrix} \underline{h}_j \\ \lambda \end{bmatrix} \tag{9.7}$$

where $\underline{x}$ are the true dynamic states, and λ are parameters.

---

[1]Tangential encounters are associated with grazing bifurcations, discussed later.
[2]Chattering is indicative of sliding mode behavior, with Filippov [7] concepts required to define solutions.

2.2   Trajectory sensitivities

Optimization and shooting method algorithms require the sensitivity of a trajectory to perturbations in parameters and/or initial conditions [10]. To obtain the sensitivity of the flow ϕ to initial conditions x_0, the Taylor series expansion of (9.6) is formed. Neglecting higher order terms gives

$$\delta x(t) = \frac{\partial x(t)}{\partial x_0} \delta x_0 \equiv \Phi(t, x_0) \delta x_0 \tag{9.8}$$

where Φ is the *sensitivity transition matrix*, or *trajectory sensitivities*, associated with the flow of x [11]. Equation (9.8) describes the change $\delta x(t)$ in a trajectory, at time t along the trajectory, for a given (small) change in initial conditions $\delta x_0 = [\delta \underline{x}_0^T \ \ \delta \lambda^T]^T$.

Along smooth sections of the trajectory (between events), the variational equations describing the evolution of the trajectory sensitivities are given by the linear time-varying system

$$\dot{\Phi} = Df_\rho(t)\Phi, \qquad \Phi(0) = I \tag{9.9}$$

where $Df \equiv \frac{\partial f}{\partial x}$ and I is the identity matrix. For large systems, these equations have high dimension. However the computational burden is minimal when an implicit numerical integration technique such as trapezoidal integration is used to generate the trajectory. Further details can be found in [12, 13, 14].

It is shown in [12] that at an event $i \rightarrow j$, occurring at time τ, the trajectory sensitivities Φ generically jump according to

$$\Phi(\tau^+, x_0) = Dh_{ij}\Phi(\tau^-, x_0) + (f_j - Dh_{ij}f_i)\frac{\nabla s_{ij}^T \Phi(\tau^-, x_0)}{\nabla s_{ij}^T f_i} \tag{9.10}$$

$$= \left(Dh_{ij} + (f_j - Dh_{ij}f_i)\frac{\nabla s_{ij}^T}{\nabla s_{ij}^T f_i} \right) \Phi(\tau^-, x_0). \tag{9.11}$$

Notice that the transversality condition (9.3) ensures that the denominator of (9.10) is non-zero.

Equation (9.10) can be rewritten

$$\Phi^+ = Dh_{ij}\Phi^- - (f_j - Dh_{ij}f_i)\frac{\partial \tau}{\partial x_0} \tag{9.12}$$

where

$$\frac{\partial \tau}{\partial x_0} = -\frac{\nabla s_{ij}^T \Phi^-}{\nabla s_{ij}^T f_i}$$

Figure 9.1.   Jump conditions.

gives the sensitivity of the event triggering time to initial conditions. Visualizing this result is easiest when $h_{ij}(x) = x$, which gives $Dh_{ij} = I$. Then for a perturbation δx_0, (9.12) gives

$$\delta x = \Phi^- \delta x_0 + f_i \delta\tau = \Phi^+ \delta x_0 + f_j \delta\tau$$

which is illustrated in Figure 9.1.

3.   Dynamic Embedded Optimization

Optimization problems arise frequently in the analysis of power system dynamics. Examples range from tuning generator AVR/PSSs [15] to determining the optimal location, amount and switching times for load shedding [16]. Many problems can be formulated using a Bolza form of objective function

$$\min_{\theta, t_f} \mathcal{J}(x, \theta, t_f) \tag{9.13}$$

$$\text{subject to}\quad x(t) = \phi(t, x_0) \tag{9.14}$$

$$x \in \mathcal{S} \qquad \text{(constraint set)} \tag{9.15}$$

where

$$\mathcal{J}(x, \theta, t_f) = \varphi\big(x(t_f), \theta, t_f\big) + \int_0^{t_f} \psi\big(x(t), \theta, t\big) dt \tag{9.16}$$

and θ are the design parameters, i.e., the parameters adjusted to achieve the objective. Adjustability of the final time t_f is problem specific. This

problem is closely related to optimal control [17], but solves for finite dimensional θ, rather than an infinite dimensional control input $u(t)$.

The solution of (9.13) for hybrid systems is complicated by discontinuous behavior at events. However those complications largely disappear under the assumption that the order of events does not change as θ and t_f vary, i.e., no grazing situations occur. This assumption is common throughout the literature, though it is expressed in various ways: transversal crossings of triggering hypersurfaces are assumed in [18], existence of trajectory sensitivities is assumed in [19], and [20] assumes all flows have the same *history*. All statements are equivalent.

Under that assumption, and other mild assumptions, it is concluded in [20] that if $\mathcal{J}$ is continuous in its arguments then a solution to (9.13) exists. Furthermore, [19] shows that if $\mathcal{J}$ is a smooth function of its arguments, then it is continuously differentiable with respect to θ and t_f. The minimization can therefore be solved using gradient-based methods. Trajectory sensitivities underlie the gradient information.

It is still an open question as to which gradient-based methods are most appropriate for solving (9.13)-(9.16). Steepest descent is simple to implement, but may require many iterations. This situation is to be avoided, as each evaluation of $\mathcal{J}$ requires simulation of the embedded dynamical system. Encouraging results have been obtained with conjugate-gradient and quasi-Newton methods [21]. A further advantage of these latter methods is that they provide an estimate of the Hessian $\partial^2 \mathcal{J}/\partial\theta^2$. (Building the true Hessian is infeasible, as it involves second order trajectory sensitivities which are computationally expensive.) The (approximate) Hessian may provide an indication of coupling between design parameters θ, and hence allow physical insights that assist in the design process.

If the event ordering assumption given above is not satisfied, $\mathcal{J}$ may be discontinuous. The optimization problem then takes on a combinatorial nature, as each continuous section of $\mathcal{J}$ must be searched for a local minimum [19].

Example Non-traditional design capabilities arise from embedding a hybrid system model within the optimization framework (9.13)-(9.16). To illustrate, consider the generator AVR/PSS shown in Figure 9.2. The clipping limits on the PSS output V_{PSS} and the anti-windup limits on the field voltage E_{fd} introduce events that result in non-smooth behavior. Typically PSS output limits are assigned on an *ad hoc* basis. However [15] determines optimal limit values by establishing a cost function (9.16) that maximize damping whilst penalizing deviations in the generator terminal voltage. Figure 9.3 compares optimal performance with that
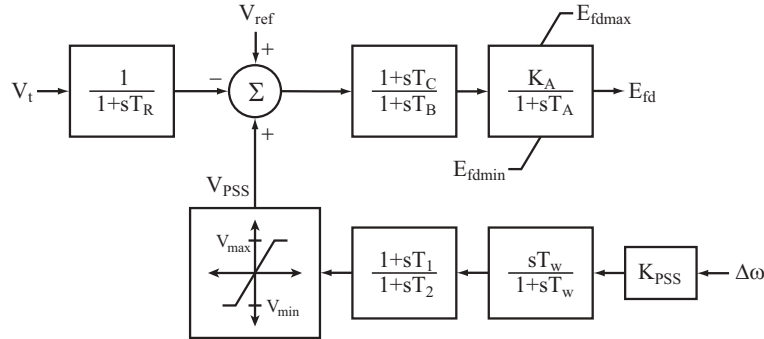
Figure 9.2. AVR/PSS block representation.

obtained using standard limit values. (Note that only the limit values differ between these two cases. All other parameters are fixed.) The underlying non-smoothness of this example is apparent from the field voltage behavior.

□

Other optimization problems do not naturally fit the Bolza form of objective function (9.16). Cascaded tap-changing transformers provide an interesting example [22]. Minimizing the number of tap change operations is equivalent to minimizing the number of crossings of triggering hypersurfaces. Such a problem, by definition, does not satisfy the earlier assumption requiring constant ordering of events.

4. Shooting Methods

Boundary value problems have the form

$$r\big(x_0, x(t_f)\big) = 0 \tag{9.17}$$

where t_f is the final time, and $x(t)$ is the trajectory that starts from x_0 and is generated by the hybrid system model (9.1). The initial values x_0 are variables that must be adjusted to satisfy r. (Though r may directly constrain some elements of x_0.) To establish the solution process, (9.17) may be rewritten

$$r\big(x_0, \phi(t_f, x_0)\big) = 0 \tag{9.18}$$

which has the form $\tilde{r}(x_0) = 0$. Boundary value problems are solved by shooting methods [10, 23], which are a combination of Newton's method for solving (9.18) along with numerical integration for obtaining the flow ϕ. Newton's method requires the Jacobian

$$J = \frac{\partial r}{\partial x_0} + \frac{\partial r}{\partial x}\Phi(t_f) \tag{9.19}$$
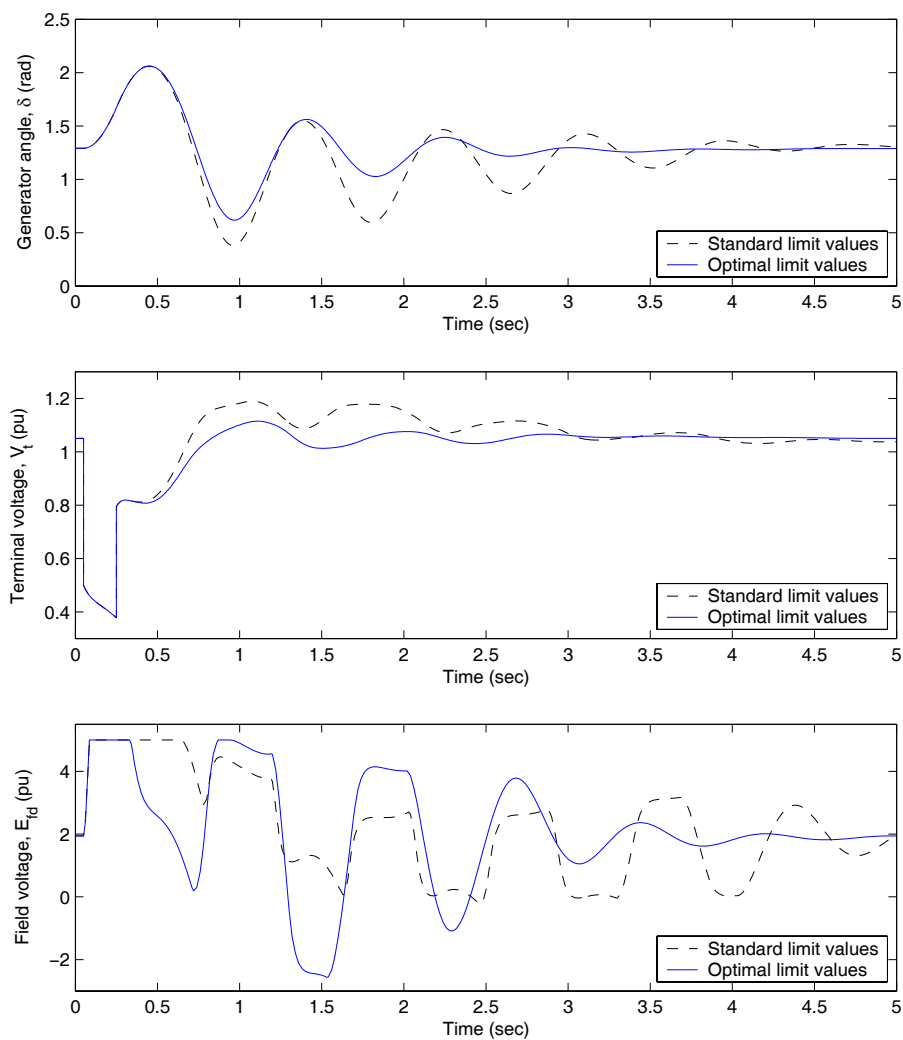
Figure 9.3. Damping improvement from optimally tuning PSS limits.

which is dependent upon the trajectory sensitivities evaluated at t_f.

Boundary value problems *per se* are uncommon in power systems. However, two applications are of increasing importance: limit cycles (sustained oscillations) and grazing phenomena. They are discussed in the following subsections.
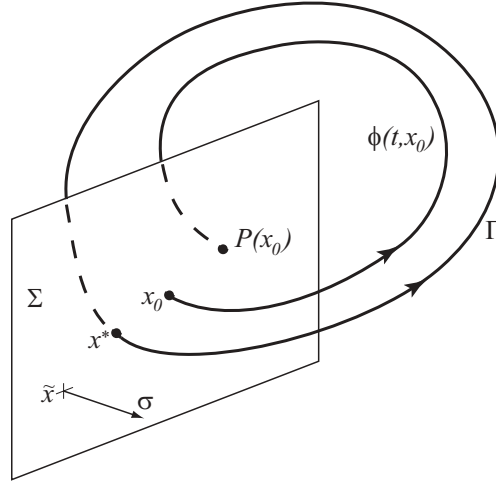
Figure 9.4.   Poincaré map.

4.1   Limit cycles

Oscillations have been observed in a variety of power systems, from generation [2] to distribution [24]. In this latter case, oscillations were driven by interactions between transformer tapping and capacitor switching. A hybrid system representation is necessary for capturing such phenomena.

Periodic behavior of limit cycles implies that the system state returns to its initial value every cycle. This can be expressed in terms of the flow as

$$x^* = \phi(T, x^*) \tag{9.20}$$

where T is the limit cycle period. For non-autonomous systems, the period T is a known quantity. However, it is not known *a priori* for autonomous systems. The unknown period, or *return time*, can be found using Poincaré map concepts [25, 23]. These concepts are well known; the following summary is provided for completeness.

Referring to Figure 9.4, let Σ be a hyperplane that is transversal to the flow $\phi(t, x_0)$, and defined by

$$\Sigma = \{x : \sigma^T (x - \tilde{x}) = 0\} \tag{9.21}$$

where $\tilde{x}$ is a point anchoring Σ and σ is a vector normal to Σ. The return time τ_r for a trajectory emanating from $x_0 \in \Sigma$ is therefore given by

$$\sigma^T (\phi(\tau_r, x_0) - \tilde{x}) = 0 \tag{9.22}$$

The flow ϕ and hyperplane Σ together describe a Poincaré map P : $\Sigma \to \Sigma$, defined by

$$P(x_0) = \phi(\tau_r(x_0), x_0) \qquad (9.23)$$

where $\tau_r(.)$ is given (implicitly) by (9.22). Therefore from (9.20), a limit cycle of an autonomous system must satisfy

$$x^* = P(x^*) = \phi(\tau_r(x^*), x^*) \qquad (9.24)$$

The corresponding limit cycle is labelled Γ in Figure 9.4.

Limit cycles can be located by solving (9.20) for non-autonomous systems or (9.24) for autonomous systems. For autonomous systems, rewriting (9.24) gives

$$F_l(x^*) = \phi(\tau_r(x^*), x^*) - x^* = 0 \qquad (9.25)$$

The solution x^* can be obtained using a shooting method[3], which solves the iterative scheme

$$x^{k+1} = x^k - \left(DF_l(x^k) \right)^{-1} F_l(x^k) \qquad (9.26)$$

where

$$DF_l(x^k) = \Phi(\tau_r(x^k), x^k) - f|_{\tau_r(x^k)} \frac{\sigma^T \Phi(\tau_r(x^k), x^k)}{\sigma^T f|_{\tau_r(x^k)}} - I \qquad (9.27)$$

$$= \left(I - \frac{f|_{\tau_r(x^k)} \sigma^T}{\sigma^T f|_{\tau_r(x^k)}} \right) \Phi(\tau_r(x^k), x^k) - I \qquad (9.28)$$

Derivation of DF_l is given in [25, 26].

As shown in Section 2.2, the sensitivity transition matrix Φ in (9.28) is well defined for hybrid systems. Therefore the proposed shooting method is suitable for non-smooth limit cycles. This will be illustrated in the later example.

Stability of limit cycles can be determined using Poincaré maps. The Poincaré map (9.23) effectively samples the flow of a periodic system once every period. If the limit cycle is stable, oscillations approach the limit cycle over time. The samples provided by the corresponding Poincaré map approach a fixed point. A non-stable limit cycle results in divergent oscillations. For such a case the samples of the Poincaré map diverge.

---

[3]Reformulation as a multiple shooting method [10] is straightforward.

Stability of the Poincaré map is determined by linearizing P at the fixed point x^*,

$$\Delta x_{k+1} = DP(x^*)\Delta x_k \qquad (9.29)$$

For autonomous systems, it follows from (9.28) that

$$DP(x^*) = \left(I - \frac{f(x^*)\sigma^T}{\sigma^T f(x^*)} \right) \Phi(\tau_r(x^*), x^*) \qquad (9.30)$$

The eigenvalues of $DP(x^*)$ are known as the *characteristic multipliers* m_i of the periodic solution. The matrix $\Phi(\tau_r(x^*), x^*)$ in (9.30) is exactly the sensitivity transition matrix after one period of the limit cycle, i.e., starting from x^* and returning to x^*. This matrix is called the *Monodromy matrix*.

It is shown in [25] that for an autonomous system, one eigenvalue of $\Phi(\tau_r(x^*), x^*)$ is always unity, and the corresponding eigenvector lies along $f(x^*)$. The remaining eigenvalues of $\Phi(\tau_r(x^*), x^*)$ coincide with the eigenvalues of $DP(x^*)$, i.e., the characteristic multipliers. These characteristic multipliers are independent of the choice of hyperplane Σ. Therefore, for hybrid systems, it is often convenient to choose Σ as a triggering hypersurface corresponding to an event that occurs along the periodic solution.

Because the characteristic multipliers m_i are the eigenvalues of the linear map $DP(x^*)$, they determine the local stability of the Poincaré map $P(.)$, and hence the local stability of the periodic solution. If all m_i lie within the unit circle, the map is locally stable, so the periodic solution is locally stable. Alternatively, if any of the m_i lie outside the unit circle, then the periodic solution is unstable.

Example　A simple single machine infinite bus system can be used to illustrate power system limit cycles. The machine is represented by a sixth order model [27], and has an AVR of the form shown in Figure 9.2, but with the PSS disabled. The system has an asymptotically stable operating point for values of AVR gain $K_A < 278$. A supercritical Hopf bifurcation [23] occurs near $K_A = 278$. For $K_A > 278$, the equilibrium point becomes unstable and a stable limit cycle appears. The amplitude of that limit cycle grows as K_A increases, with the maximum field voltage limiter becoming active for $K_A > 294$.

The limit cycle corresponding to $K_A = 300$ is shown in Figure 9.5, as a plot of field voltage E_{fd} versus terminal voltage V_t. Notice that the limit cycle is non-smooth due to the field voltage limit $E_{fd,max} = 5$ p.u.

For this case the eigenvalues of the Monodromy matrix are 1, 0.84, $0.21 \pm j0.25$, 0.08 and four at 0. The unity eigenvalue is always present for
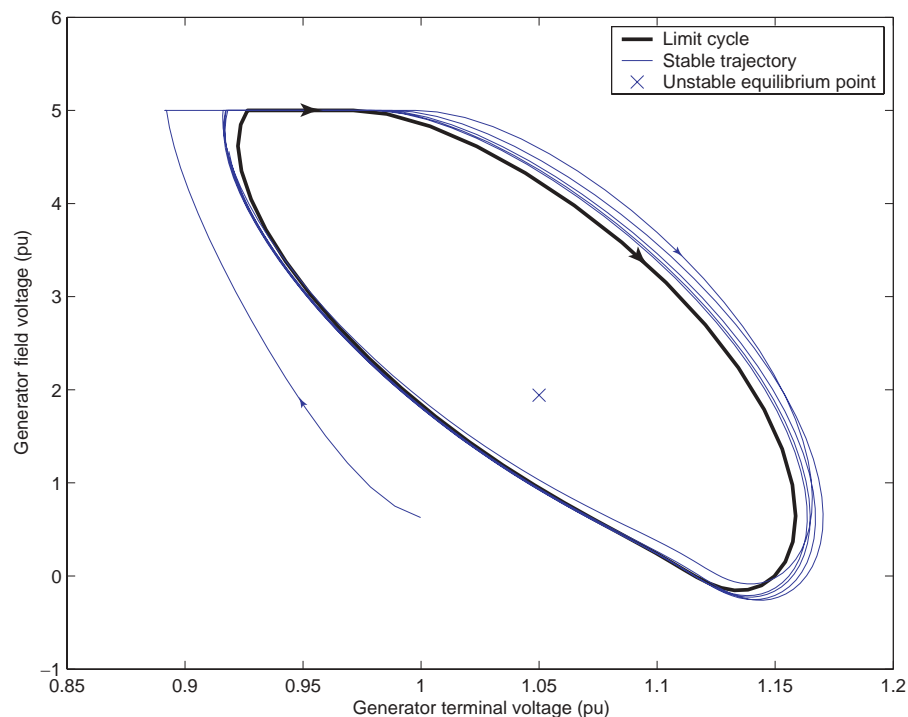
Figure 9.5. Non-smooth limit cycle.

autonomous systems, as suggested by the theory. The other eigenvalues are the characteristic multipliers for this limit cycle. Notice that one of the characteristic multipliers is relatively close to unity, indicating that the limit cycle is quite poorly damped. Indeed the non-equilibrium trajectory in Figure 9.5 converges slowly to the limit cycle.

Even though it is theoretically possible to obtain this limit cycle by simulation, slow convergence makes the process impractical. On the other hand, shooting method convergence properties follow from the underlying Newton solution process, rather than from the behavior of the dynamical system. For this example, the shooting method was initialized at the unstable equilibrium point corresponding to $K_A = 300$, except that the angle state was perturbed slightly. Convergence was obtained in eight iterations from this onerous initialization.
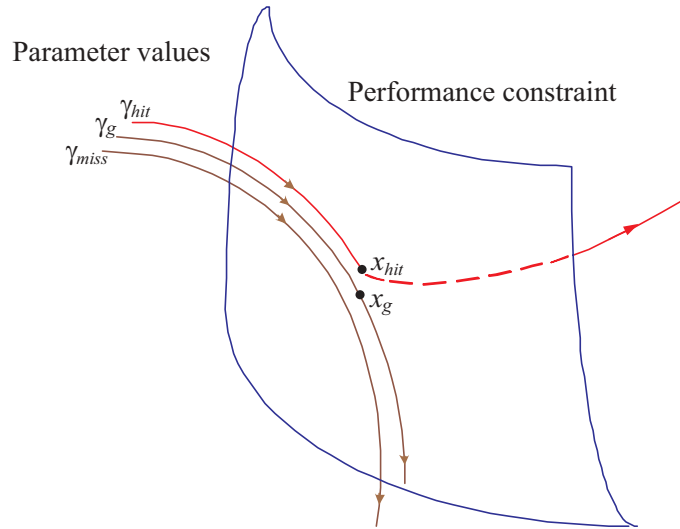
Figure 9.6.   Grazing phenomenon.

4.2   Grazing phenomena

As suggested in Section 1, if a system trajectory encounters the operating characteristic of a protection device, a trip signal is sent to circuit breakers. If the trajectory almost touches the operating characteristic but just misses, no trip signal is issued. The bounding (separating) case corresponds to the trajectory grazing, i.e., just touching, the operating characteristic, but not crossing it. Under certain circumstances, this is referred to as a *grazing bifurcation* [28, 29]; it separates two cases that have significantly different forms of behavior.

Figure 9.6 provides a more general picture. For a certain value of parameter γ_{hit}, the system trajectory encounters a performance constraint[4] at a point x_{hit}. An event occurs, and the trajectory continues accordingly. However, for a small change in parameter value, to γ_{miss}, the trajectory misses (at least locally) the constraint and subsequently exhibits a completely different form of response. At a critical parameter value γ_g, lying between γ_{hit} and γ_{miss}, the trajectory tangentially encounters (*grazes*) the constraint. Behavior beyond the grazing point x_g is generally unpredictable, in the sense that without further knowledge of the system, it is impossible to determine whether or not the event triggers.

---

[4]This may be a protection operating characteristic, or some other constraint established to ensure adequate system performance.

Grazing is characterised by a trajectory (flow) of the system touching a triggering hypersurface tangentially. Let the target hypersurface be described by

$$b(x) = 0 \qquad (9.31)$$

where $b : \mathbb{R}^n \to \mathbb{R}$. Vectors that are normal to b are therefore given by $\nabla b = (\partial b/\partial x)^T$, and the tangent hyperplane is spanned by vectors u that satisfy $\nabla b^T u = 0$. The vector $\dot{x} = f(x)$ is directed tangentially along the flow, so at a grazing point

$$\nabla b^T f(x) = 0 \qquad (9.32)$$

A single degree of freedom is available for varying parameters to find a grazing point. Recall from (9.7) that parameters λ are incorporated into the initial conditions x_0. Therefore the single degree of freedom can be achieved by parameterization $x_0(\theta)$, where θ is a scalar.

Grazing points are therefore described by combining together the flow definition (9.6) (appropriately parameterized by θ), target hypersurface (9.31), and tangency condition (9.32), to give

$$
\begin{align}
F_{g1}(x_g, \theta, t_g) &:= \phi(t_g, x_0(\theta)) - x_g = 0 & (9.33) \\
F_{g2}(x_g) &:= b(x_g) \quad\quad\quad\quad = 0 & (9.34) \\
F_{g3}(x_g) &:= \nabla b(x_g)^T f(x_g) \quad = 0 & (9.35)
\end{align}
$$

Grazing occurs at time t_g along the trajectory, and its state-space location is given by x_g. This set of equations may be written compactly as

$$F_g(x_g, \theta, t_g) = F_g(z) = 0 \qquad (9.36)$$

where $F_g : \mathbb{R}^{n+2} \to \mathbb{R}^{n+2}$ and $z = [x_g^T \; \theta \; t_g]^T$.

Numerical solution of (9.36) using Newton's method amounts to iterating on the standard update formula

$$z^{k+1} = z^k - \left(DF_g(z^k)\right)^{-1} F_g(z^k) \qquad (9.37)$$

where DF_g is the Jacobian matrix

$$DF_g = \begin{bmatrix} -I & \Phi\frac{dx_0}{d\theta} & f \\ \nabla b^T & 0 & 0 \\ f^T\nabla^2 b + \nabla b^T Df & 0 & 0 \end{bmatrix} \qquad (9.38)$$

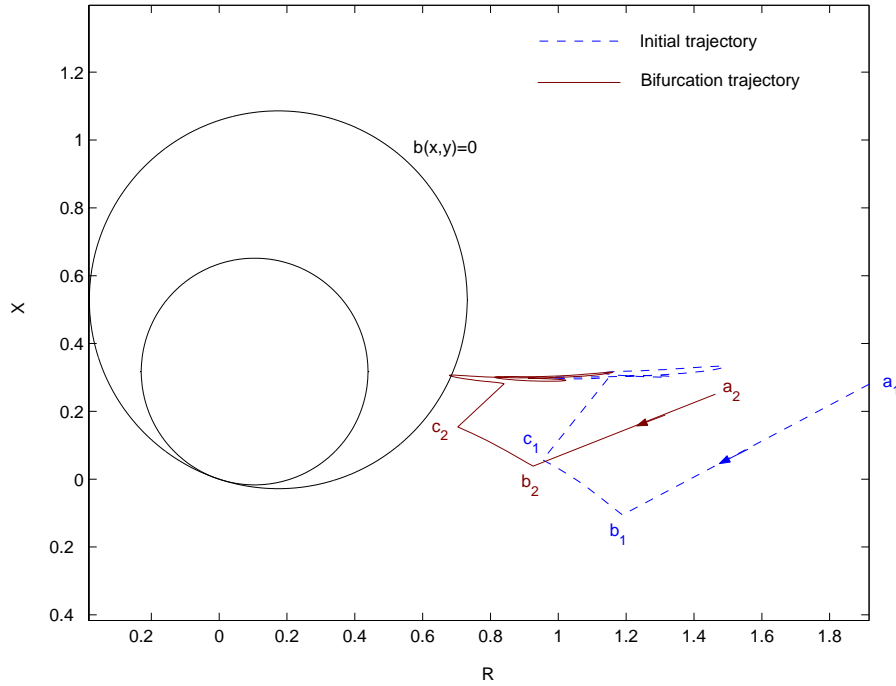More complete details of this algorithm are given in [26].

Figure 9.7.   Impedance plane trajectories.

Example   An example of grazing is presented in Figure 9.7, where zone 1 and 2 operating characteristics for a distance protection relay appear as circles in the impedance plane. The dashed line, which begins at the pre-fault operating point a_1, shows the system response to a disturbance for nominal system conditions. At the onset of the fault, the apparent impedance jumps from a_1 to b_1. It then evolves to c_1 during the fault-on period. At fault clearing, the apparent impedance jumps, approaches the zone 2 characteristic, then turns away. Under these nominal conditions the relay characteristic is not encountered.

As load increases, the impedance trajectory moves closer to the relay characteristic. The example considered the load increase required for the relay characteristic to be encountered. This established the maximum secure loading level. The problem was formulated according to (9.33)-(9.35), with b describing the zone 2 operating characteristic, and θ giving the load deviation. Convergence of (9.37) was obtained in four iterations, with the grazing trajectory shown as the solid curve in Figure 9.7. The load change moved the pre-fault operating point from a_1 to a_2. As required, this trajectory just touches the relay characteristic.

5.   Challenges in Dynamic Performance Enhancement

Power systems are becoming increasingly complex. Trends include greater utilization of special protection schemes, FACTS devices, and distributed resources. (Market dynamics may also become influential as the associated time-constants diminish.) These newer influences, together with operation closer to limits, is resulting in a greater level of switching (non-smooth) activity. The techniques proposed in this paper are suited to such hybrid behavior. However more work is required. Hybrid dynamics introduce new challenges for control design. For example, minimization of switching events does not fit a normal optimization framework [30]. Also, assessment of stability limits is technically difficult [31].

Distributed resources, such as small generation sources, newer FACTS technology [32], and load control [33, 34], individually exert negligible influence on dynamic behavior. However collectively their effect may be significant. Modelling of each device is impossible, so techniques for aggregating behavior and handling the associated model uncertainty will become vital for meaningful assessment of dynamics. Monte Carlo techniques are impractical, due to the computational burden of repeated simulations. Emerging practical techniques build on probabilistic collocation [35] and trajectory approximation [36]. Further work is required though.

6.   Conclusions

The response of power systems to large disturbances often involves interactions between continuous dynamics and discrete events. Power systems therefore provide an important application area for hybrid systems. Systematic modelling of hybrid systems facilitates efficient computation of trajectory sensitivities. The variational equations describing the evolution of trajectory sensitivities through events are well defined, even though the underlying behavior may be non-smooth.

Many design questions associated with enhancement of power system dynamic performance can be formulated as dynamic embedded optimization problems. Such problems are constrained to satisfy system dynamics, and so are closely related to optimal control. If the ordering of events remains fixed as parameters vary, the cost function is smooth, even though underlying dynamic behavior may be non-smooth. Gradient-based algorithms are appropriate, with trajectory sensitivities providing the gradient information. Changes in event ordering may how-

ever result in non-smoothness or even discontinuities in the cost function. In that case, a combinatorial optimization process may be required.

In contrast to design, analysis questions often take the form of boundary value problems, which can be solved using shooting methods. Limit cycles provide an example. Smooth and non-smooth limit cycles have been observed in power systems. Furthermore, unstable limit cycles often partially bound the region of stable operation. All limit cycles, whether stable or unstable, smooth or non-smooth, can be obtained reliably using shooting methods.

Power system performance constraints seek to achieve appropriate post-fault response by bounding behavior away from undesirable regions of state space. An indication of system vulnerability can therefore be obtained by determining trajectories that tangentially encounter (graze) those constraints, i.e., by pushing the system to the limit. The conditions governing such grazing trajectories take the form of a boundary value problem, which can be solved via a shooting method.

Acknowledgements

References

[1] U.S.-Canada Power System Outage Task Force. *Final Report on the August 14, 2003 Blackout in the United States and Canada: Causes and Recommendations*. April 2004.

[2] K. Kim, H. Schättler, V. Venkatasubramanian, J. Zaborszky, and P. Hirsch. Methods for Calculating Oscillations in Large Power Systems. *IEEE Transactions on Power Systems*, 12:1639–1648, 1997.

[3] G. Rogers. *Power System Oscillations*. Kluwer Academic Publishers, Norwell, MA, 2000.

[4] L.G. Perez, A.J. Flechsig, and V. Venkatasubramanian. Modeling the Protective System for Power System Dynamic Analysis. *IEEE Transactions on Power Systems*, 9:1963–1973, 1994.

[5] M.S. Ćalović. Modeling and Analysis of Under-Load Tap-Changing Transformer Control Systems. *IEEE Transactions on Power Apparatus and Systems*, PAS-103:1909–1915, 1984.

[6] M.D. Lemmon, K.X. He, and I. Markovsky. Supervisory Hybrid Systems. *IEEE Control Systems Magazine*, 19:4:42–55, August 1999.

[7] A.F. Filippov. *Differential Equations with Discontinuous Righthand Sides*. Kluwer Academic Publishers, The Netherlands, 1988.

[8] D. Liberzon. *Switching in Systems and Control.* Birkhäuser, Boston, MA, 2003.

[9] I.A. Hiskens. Power System Modeling for Inverse Problems. *IEEE Transactions on Circuits and Systems I*, 51:539–551, 2004.

[10] J. Stoer and R. Bulirsch. *Introduction to Numerical Analysis*, 2nd edition. Springer, New York, 1993.

[11] P.M. Frank. *Introduction to System Sensitivity Theory.* Academic Press, New York, 1978.

[12] I.A. Hiskens and M.A. Pai. Trajectory Sensitivity Analysis of Hybrid Systems. *IEEE Transactions on Circuits and Systems I*, 47:204–220, 2000.

[13] W.F. Feehery, J.E. Tolsma, and P.I. Barton. Efficient Sensitivity Analysis of Large-Scale Differential-Algebraic Systems. *Applied Numerical Mathematics*, 25:41–54, 1997.

[14] S. Li, L. Petzold, and W. Zhu. Sensitivity Analysis of Differential-Algebraic Equations: A Comparison of Methods on a Special Problem. *Applied Numerical Mathematics*, 32:161–174, 2000.

[15] I.A. Hiskens. Systematic Tuning of Nonlinear Power System Controllers. *Proceedings of the 2002 IEEE International Conference on Control Applications*, 19–24, Glasgow, Scotland, September 2002.

[16] C. Moors and T. Van Cutsem. Determination of Optimal Load Shedding Against Voltage Instability. *Proceedings of the 13th Power Systems Computation Conference*, 2:993–1000, Trondheim, Norway, June 1999,

[17] F.L. Lewis and V.L. Syrmos. *Optimal Control*, 2nd edition. Wiley, New York, 1995.

[18] M.S. Branicky, V.S. Borkar, and S.K. Mitter. A Unified Framework for Hybrid Control: Model and Optimal Control theory. *IEEE Transactions on Automatic Control*, 43:31–45, 1998.

[19] S. Galán and P.I. Barton. Dynamic Optimization of Hybrid Systems. *Computers Chemical Engineering*, 22:S183–S190, 1998.

[20] B. Piccoli. Hybrid Systems and Optimal Control. *Proceedings of the 37th IEEE Conference on Decision and Control*, Tampa, FL, December 1998.

[21] J. Nocedal and S.J. Wright. *Numerical Optimization.* Springer-Verlag, New York, 1999.

[22] M. Larsson. *Coordinated Voltage Control in Electric Power Systems.* PhD Thesis, Department of Industrial Electrical Engineering and Automation, Lund Institute of Technology, Lund, Sweden, 2000.

[23] R. Seydel. *Practical Bifurcation and Stability Analysis*. Springer-Verlag, New York, 1994.

[24] P. Gavey. Voltage Stability in the Mid North Coast: Investigation of Voltage Oscillation Occurrence on 26th March 1993. Final Year Project Report, Department of Electrical and Computer Engineering, The University of Newcastle, Australia, 1995.

[25] T.S. Parker and L.O. Chua. *Practical Numerical Algorithms for Chaotic Systems*. Springer-Verlag, New York, NY, 1989.

[26] V. Donde and I.A. Hiskens. Shooting Methods for Locating Grazing Phenomena in Hybrid Systems. *International Journal of Bifurcation and Chaos*, 2004, Submitted.

[27] P.W. Sauer and M.A. Pai. *Power System Dynamics and Stability*. Prentice Hall, Upper Saddle River, NJ, 1998.

[28] M.H. Fredriksson and A.B. Nordmark. Bifurcations Caused by Grazing Incidence in Many Degrees of Freedom Impact Oscillators. *Proceedings of Royal Society London A*, 453:1961:1261–1276, 1997.

[29] M. di Bernardo, C.J. Budd, and A.R. Champneys. Grazing and Border-Collision in Piecewise-Smooth Systems: A Unified Analytical Framework. *Physical Review Letters*, 86:2553–2556, 2001.

[30] R.W. Brockett. Minimum attention control. *Proceedings of the 36th IEEE Conference on Decision and Control*, 2628–2632, 1997.

[31] V. Venkatasubramanian, H. Schättler, and J. Zaborszky. Dynamics of Large Constrained Nonlinear Systems—a Taxonomy Theory. *Proceedings of the IEEE*, 83:1530–1561, 1995.

[32] D. Divan. Smart Wires: Demonstration of a Distributed Static Series Compensator (DSSC) Module. SoftSwitching Technologies Presentation, Middleton, WI, March 2004.

[33] B. Ramanathan and V. Vittal. A Structured Singular Value Based Small Signal Stability Performance Boundary for Direct Load Control. *Proceedings of IEEE Power Systems Conference and Exposition (PSCE)*, New York, October 2004 (to appear).

[34] I.A. Hiskens and B. Gong. Voltage Stability Enhancement via Model Predictive Control of Load. *Proceedings of the Symposium on Bulk Power System Dynamics and Control VI*, Cortina d'Ampezzo, Italy, August 2004 (to appear).

[35] J.R. Hockenberry and B.C. Lesieutre. Evaluation of Uncertainty in Dynamic Simulations of Power System Models I: the Probabilistic Collocation Method. *IEEE Transactions on Power Systems*, 19:1483–1491, 2004.

[36] I.A. Hiskens, M.A. Pai, and T.B. Nguyen. Bounding Uncertainty in Power System Dynamic Simulations. *Proceedings of IEEE PES Winter Meeting*, Singapore, January 2000.